Diffractive Higgs boson production at the Tevatron and the LHC

Christophe Royon*

Abstract

We evaluate inclusive Higgs boson and dijet cross-sections at the Tevatron and the LHC colliders via double Pomeron exchange allowing for the presence of Pomeron remnants. Sizeable cross-sections and encouraging event selection signals are found for the LHC, demonstrating especially for small Higgs boson masses the importance to study the diffractive channels. Tagging of the Pomeron remnants can be exploited to achieve a good resolution on the Higgs mass for inclusive diffractive events, by optimizing an analysis between higher cross-sections of the *inclusive* mode (all Pomeron remnants) and cleaner signals of the *exclusive* mode (without Pomeron remnants).

1 Introduction

It has been suggested [1, 2] that diffractive Higgs boson production via Double Pomeron Exchange (DPE) is an interesting channel to study the Higgs boson at hadron colliders. Recently [3], the possibility of a better determination of the cross-sections and event rates was proposed. The model provides a joint description of Higgs boson production and of the observed high mass dijet production at the Tevatron (run I) [4], allowing to compare and normalize the predictions to the data using a (simplified) simulation of the detector. One important difference with previous (purely *exclusive*) estimates lies on the consideration of *inclusive* production $pp \to p + X + H + Y + p$, see Fig. 1, namely with particles accompanying the Higgs/dijet production in the central region. We will call X, Y the "Pomeron remnants" in the following. The presence of the Pomeron remnants is vital for the good description of the dijet mass spectrum as discussed in [3].

*CEA/DSM/DAPNIA/SPP, CE-Saclay, F-91191 Gif-sur-Yvette Cedex, France

2 Theoretical framework

Let us introduce the formulae for *inclusive* Higgs boson production cross-sections [1] via DPE [3]:

$$d\sigma_H^{incl} = C_H \left(\frac{x_1^g x_2^g s}{M_H^2}\right)^{2\epsilon} \delta\left(\xi_1\xi_2 - \frac{M_H^2}{x_1^g x_2^g s}\right) \prod_{i=1,2} \left\{ G_P(x_i^g,\mu)\, dx_i^g d^2v_i\, \frac{d\xi_i}{1-\xi_i}\, \xi_i^{2\alpha' v_i^2}\, \exp\left(-2v_i^2\lambda_H\right)\right\}, \quad (1)$$

where x_1^g, x_2^g define, on each side (see Fig.1), the fraction of the Pomeron's momentum carried by the gluons involved in the hard process and $G_P(x_{1,2}^g,\mu)$, is, up to a normalization, the gluon structure function in the Pomeron extracted [5] from HERA experiments; μ^2 is the hard scale (for simplicity kept fixed at 75GeV^2, the highest value studied at HERA).

The formulae (1) are written for a Higgs boson of mass M_H. The Pomeron trajectory is $\alpha(t) = 1 + \epsilon + \alpha' t$ ($\epsilon \sim .08, \alpha' \sim .25\ GeV^{-2}$), $\xi_{1,2}$ (< 0.1) are the Pomeron's fraction of longitudinal momentum, $v_{1,2}$, the 2-transverse momenta of the outgoing $p\bar{p}$, $k_{1,2}$ those of the outgoing quark jets, $\lambda_H \sim 2\ GeV^{-2}$ the slope of the non perturbative coupling for the Higgs boson, and the constant C_H is a normalization including a non-perturbative gluon coupling [1], appreciably cancelled in the ratio C_H/C_{JJ}.

The dijet cross-section [3] depends on the $gg \to \bar{Q}^f Q^f$ and $gg \to gg$ cross-sections [6].

The physical origin of formulae (1) is the following: since the overall partonic configuration is produced initially by the long-range, soft DPE interaction, we assume that, up to a normalization, the *inclusive* cross-section is the convolution of the "hard" *partons* $\to$ *Higgs boson*, (or *partons* $\to$ *jets*) subprocesses by the Pomeron structure function into gluons, see Fig.1. The expected factorization breaking of hadroproduction will appear in the normalization through a renormalization of the Pomeron fluxes, which are not the same as in hard diffraction at HERA.

3 Predictions for the Tevatron

3.1 Comparison with the CDF run I measurement

Let us compare our results with the measurements performed in the CDF experiment at Tevatron [4]. To this end, we interfaced our generator with `SHW` [7] a fast simulation of the D0 and CDF detectors. We chose as gluon content of the Pomeron the result of the H1 "fit 1" performed in Ref. [5], up to a normalization of the flux determined by comparison with CDF results.

We first compared our results for the dijet mass fraction with the measurement of the CDF collaboration [4] in double Pomeron events (see Fig.2 in the first reference of Ref. [3]). The dijet mass fraction spectrum is well reproduced if radiation (namely the promeron remnants) is introduced.

[1] The same formalism gives formulae for dijet, diphoton and dilepton production, see [3].

To be more detailed, a tagged antiproton with $0.035 \leq \xi_{\bar{p}} \leq 0.095$ and $|t| < 1$ GeV^2 was required. This quantity is reconstructed using the roman pot detectors installed by the CDF collaboration. To get correct predictions for the Higgs boson production cross section cross sections at the Tevatron and the LHC in the following, we adjusted our dijet cross section to the CDF Run I measurement.

3.2 Diffractive Higgs boson cross section at the Tevatron

We can now give predictions for the Higgs boson production cross sections in double diffractive events at the generator level and after a fast simulation of the detector. The results are given in Table 1. We note the low values of the cross-sections [2].

4 Predictions for the LHC

4.1 Higgs boson production cross section at the LHC

We can now give predictions for the Higgs boson production cross sections in DPE events at the LHC. The results are given in Table 2 (first column) and in Fig. 2. We note the high values of the cross-sections. Since the typical luminosity for the LHC will be of the order of 10-100 fb^{-1}/year, this leads to several thousand Higgs particles diffractively produced per year, even at low luminosity. Hence for the inclusive channel the cross section is large, much larger than recent calculations for the exclusive channel (see Ref.[8]-b). In Ref.[8]-a, similar conclusions are reached (note however [8]-c).

In Fig. 2, we show the effects of the acceptance of the possible roman pots detectors at the LHC, which are used in conjunction with a central detector. As an example, following ideas presently discussed in a common study group of the central detector CMS [9] and the elastic/soft diffraction experiment TOTEM [10], which both will use the same interaction region at the LHC, we choose four possible configurations for roman pot detectors to measure the scattered protons. The used acceptance numbers are based on [11]. The first one (see, *Config.1* on Fig.2) has roman pot detectors located in the warm region of the LHC respectively at 140-180 meters and 240 meters and assumes a good acceptance for protons with $|t| < 2$ GeV^2, and $\xi > 0.01$. The second one (*Config.2*) considers only roman pots at 140-180 meters [10] and gives a good acceptance only for $|t| < 1.5$ GeV^2, and $\xi > 0.02$. *Config.3* assumes the presence of roman pot detectors in the cold region of the LHC at about 425 meters and gives a good acceptance for $|t| < 2$ GeV^2, and $0.002 < \xi < 0.02$. Certainly the latter will be challenging both from the machine and experimental point of view, but Fig.2 demonstrates that such detectors are needed to obtain a good acceptance for low mass Higgs production. *Config.4* corresponds to the full system using all detectors. In Table 1, the acceptance of the roman pot detectors in the case of *Config.4* is taken into account, and we give the number of events for 10 fb^{-1} in the different Higgs decay modes.

[2] The expected luminosity is about 15 fb^{-1} per experiment for run II.

4.2 Higgs boson mass reconstruction

The advantage of DPE events with respect to standard Higgs boson production lies in offering a potential to reconstruct the Higgs particle parameters more precisely. For example, one can hope to obtain a very precise Higgs mass reconstruction if one can tag and measure both the protons in the roman pot detectors as well as the Pomeron remnants.

$M_{Higgsboson}$	(1)	(2)	(3)	(4)	(5)
100	7.7	5.2	1.6	0.5	0.0
110	4.7	2.9	1.3	0.3	0.1
120	2.7	1.5	0.8	0.1	0.3
130	1.4	0.6	0.4	0.0	0.4
140	0.6	0.1	0.1	0.0	0.3

Table 1: Number of Higgs boson events for 1 fb^{-1}. The first column gives the number of events at the generator level (all decay channels included), and the other columns after a fast simulation of the detector. The second colum gives the number of events decaying into $b\bar{b}$ tagged in the dipole roman pot detectors of the DØ Collaboration, the third one requiring additionally at least two jets of $p_T > 30GeV$, the fourth one gives the number of reconstructed and tagged events when the Higgs boson decays into τ, and the fifth one when the Higgs boson decays into W^+W^- (in this channel, the background is found to be negligible).

$M_{Higgsboson}$	(1)	(2)	(3)	(4)	(5)	(6)
120	3219	2043	228	447	48	0
150	2637	417	48	1827	222	0
200	1995	3	0	1470	522	0
300	1419	0	0	984	438	0
375	1674	0	0	1047	483	138

Table 2: *Number of Higgs boson events for 10 fb^{-1}.* The first column gives the number of events at the generator level (all decay channels included), and the other columns take into account the roman pot acceptance and give the number of events for different Higgs boson decay channels (2: $b\bar{b}$, 3: $\tau^+\tau^-$, 4: WW, 5: ZZ, 6: $t\bar{t}$,).

In Fig. 3, we describe the results of the Higgs boson mass reconstruction assuming one is able to select and measure the Pomeron remnants (the CMS collaboration has a project to put some detectors at very high rapidity up to 7.5). The Higgs boson mass can be reconstructed by applying quadri-momentum conservation to all particles in the final state, namely the Higgs boson, the scattered protons in the roman pot detectors, and the Pomeron remnants. The energy $E = \sqrt{\xi_1\xi_2 s}$ [12] is used to produce the Higgs boson and

the Pomeron remnants.

The quality of the reconstruction of the remnants needs to be demonstrated after including hadronization and detector effects, and are subject to a future detailed study. Meanwhile we assume it can be done with a resolution of $100\%/\sqrt{E}$ (resp. $300\%/\sqrt{E}$) in an optimistic (resp. more pessimistic) scenario.

In Fig. 3, we display the resolution (resp. 2.1, 4.0, 4.6 and 6.6 GeV) on the Higgs boson mass reconstruction for four different cuts on the Pomeron remnant energy (resp. 20, 50, 100 and 500 GeV) and for the optimistic scenario. The plot with the best resolution (2.1 GeV) is shown for a luminosity of 30 fb^{-1}. In the more pessimistic scenario, the resulting Higgs mass resolution is about 7 GeV for a 120 GeV Higgs. A good coverage in pseudo-rapidity will be essential to be able to precisely measure the Higgs boson parameters. Note that the events showing little energy for the Pomeron remnants have a low value of ξ, since $M_H \sim \sqrt{\xi_1 \xi_2 s}$, which leads to $\xi_1 \xi_2 \sim 7.10^{-5}$. Hence roman pot detectors in the region of about 400 m from the interaction point will be essential.

At the LHC it is also important to consider background events. We determined that the signal over background ratio is enhanced compared to the non diffractive case because of the good resolution on the dijet mass and the cut on the mass window. Initial studies indicate that the $b\bar{b}$ channel will be interesting to look for Higgs in the diffractive mode. A full study will require a detailed simulation of the detectors and will be performed in a near future. We also give in Table I the number of events in the τ channel where the background is found to be negligible, and thus is also a promising channel even if the cross section is smaller. To summarize, the $b\bar{b}$ and $\tau^+\tau^-$ Higgs boson decays are of particular interest for low mass diffractive Higgs production because of mass resolution and background rejection. Diffractively produced Higgs bosons at higher masses are less interesting because of the clear signal already expected in the ZZ channel in standard production.

To summarize, we have shown that the diffractive inclusive Higgs production leads to large event rates at the LHC. A Higgs mass reconstruction with good precision is possible if both protons in the final state can be tagged with roman pot detectors and if the Pomeron remnants can be measured in the forward region with sufficient resolution. This channel and method will be especially useful in the low mass Higgs region where the standard methods for Higgs measurements at the LHC are challenging.

Acknowledgments

These results have been obtained from a fruitful collaboration with M. Boonekamp, A. De Roeck, and R. Peschanski.

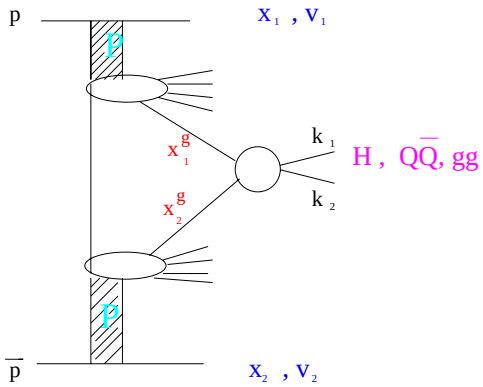

Figure 1: Production scheme. $x_i \equiv 1–\xi_i, v_i$ are the longitudinal and transverse 2-momenta of the diffracted (anti)proton (see formula (1) and text for the other kinematical notations).

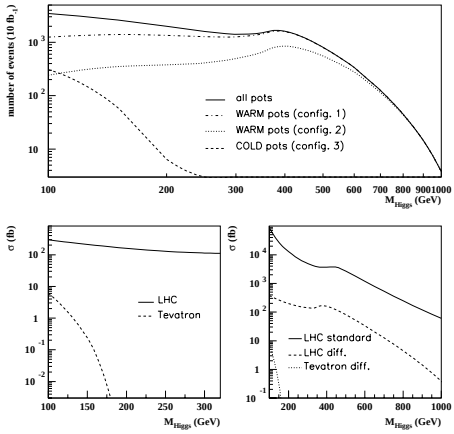

Figure 2: Diffractive Higgs boson production cross section. *Upper plot*: number of Higgs boson events for 10 fb^{-1} as a function of M_H obtained for different roman pot configurations (see text). *Bottom plots*: Diffractive Higgs boson production cross section as a function of M_H for the LHC (and the Tevatron). The standard inclusive Higgs boson production cross section is also shown for comparison.

References

[1] A. Bialas and P.V. Landshoff, *Phys. lett.* **B256** (1990) 540, A. Bialas and W. Szeremeta, *Phys. lett.* **B296** (1992) 191, A. Bialas and R. Janik, *Zeit. für. Phys.* **C62** (1994) 487.

[2] A. Schafer, O. Nachtmann, and R. Schöpf, *Phys. lett.* **B249** (1990) 331, J.D. Bjorken, *Phys.Rev.* **D47** (1993), J-R Cudell and O.F. Hernandez, *Nucl. Phys.* **B471** (1996) 471; H.J. Lu, J. Milana *Phys.Rev.* **D51** (1995) 6107; D. Graudenz, G. Veneziano *Phys. lett.* **B365** (1996) 302; M. Heyssler, Z. Kunszt, and W.J. Stirling, *Phys. lett.*

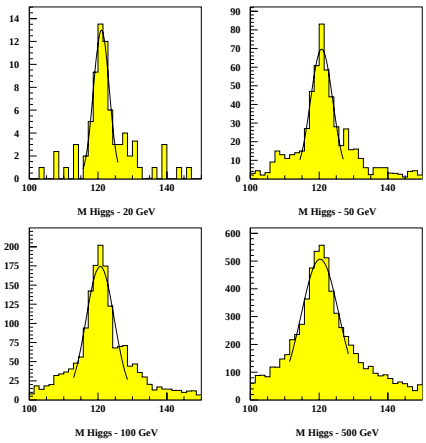

Figure 3: Higgs mass resolution. The resolution on the Higgs boson mass is shown after four different cuts on the Pomeron remnant energies at 20, 50, 100 and 500 GeV for a luminosity of 30 fb^{-1}.

B406 (1997) 95; E.M. Levin, hep-ph/9912403 and references therein; V.A. Khoze, A.D. Martin, and M.G. Ryskin, *Eur.Phys.J.* **C14** (2000) 525, *id.* **C19** (2001) 477, hep-ph/0006005; V.A. Khoze, hep-ph/0105224.

[3] M. Boonekamp, R. Peschanski, and C. Royon, *Phys. Rev. Lett.* **87** (2001) 251806, M. Boonekamp, R. Peschanski, A. De Roeck and C. Royon, Phys. Lett., in press.

[4] T. Affolder et al. , CDF Coll. , *Phys. Rev. Lett.* **85** (2000) 4215.

[5] C. Royon, L. Schoeffel, J.Bartels, H.Jung, and R.Peschanski, *Phys. Rev.* **D63** (2001) 074004.

[6] B.L. Combridge and C.J. Maxwell, *Nucl. Phys.* **B239** (1984) 429.

[7] *SHW, a fast simulation package for D0 and CDF detectors*, see `www.physics.rutgers.edu/jconway/soft/shw/shw.html`.

[8] -a B. Cox, J. Forshaw, and B. Heinemann, *Phys. lett.* **B540** (2002) 263,;
-b Similar conclusion but mainly for *exclusive* production: V.A. Khoze, A.D. Martin, and M.G. Ryskin, *Eur.Phys.J.* **C24** (2002) 581.
-c Model using a different (non Pomeron) mechanism favoring single diffractive over DPE Higgs production at the LHC: R. Enberg, G. Ingelman, A. Kissavos, and N. Timneanu,*Phys. Rev. Lett.* **89** (2002) 081801.

[9] CMS Collab., Technical Design Report (1997).

[10] TOTEM Collab., Technical Design Report, preprint CERN/LHCC 99-7.

[11] R. Orava, talk at LISHEP02, Rio de Janeiro, February 2002.

[12] M.G. Albrow and A. Rostovtsev, hep-ph/0009336.